HHS Public Access

Author manuscript

Neuroimage. Author manuscript; available in PMC 2020 October 01.

Published in final edited form as:

Neuroimage. 2020 October 01; 219: 117043. doi:10.1016/j.neuroimage.2020.117043.

Functional brain connectivity in ex utero premature infants compared to in utero fetuses

Josepheen De Asis-Cruz[a], **Kushal Kapse**[a], **Sudeepta K. Basu**[b], **Mariam Said**[b], **Dustin Scheinost**[c], **Jonathan Murnick**[a], **Taeun Chang**[d], **Adre du Plessis**[e], **Catherine Limperopoulos**[a,f,*]

[a]Diagnostic Imaging and Radiology, Children's National, Washington, DC, USA

[b]Neonatology, Children's National, Washington, DC, USA

[c]Radiology and Biomedical Imaging, Statistics and Data Science, and Child Study Center, Yale School of Medicine, New Haven, CT, USA

[d]Neurology, Children's National, Washington, DC, USA

[e]Fetal Medicine Institute, Children's National, Washington, DC, USA

[f]Pediatrics, The George Washington University School of Medicine, Washington, DC, USA

Abstract

Brain structural changes in premature infants appear before term age. Functional differences between premature infants and healthy fetuses during this period have yet to be explored. Here, we examined brain connectivity using resting state functional MRI in 25 very premature infants (VPT; gestational age at birth <32 weeks) and 25 healthy fetuses with structurally normal brain MRIs. Resting state data were evaluated using seed-based correlation analysis and network-based statistics using 23 regions of interest (ROIs) per hemisphere. Functional connectivity strength, the Pearson correlation between blood oxygenation level dependent signals over time across all ROIs, was compared between groups. In both cohorts, connectivity between homotopic ROIs showed a decreasing medial to lateral gradient. The cingulate cortex, medial temporal lobe and the basal ganglia shared the strongest connections. In premature infants, connections involving superior temporal, hippocampal, and occipital areas, among others, were stronger compared to fetuses. Premature infants showed stronger connectivity in sensory input and stress-related areas

*Corresponding author. Children's National Health System, 111 Michigan Ave. N.W, Washington, DC. 20010, USA. climpero@childrensnational.org (C. Limperopoulos).

CRediT authorship contribution statement

Josepheen De Asis-Cruz: Conceptualization, Methodology, Software, Formal analysis, Investigation, Data curation, Writing - original draft, Writing - review & editing, Visualization. **Kushal Kapse**: Investigation, Resources, Data curation, Writing - review & editing. **Sudeepta K. Basu**: Resources, Writing - review & editing. **Mariam Said**: Resources, Writing - review & editing. **Dustin Scheinost**: Methodology, Software, Writing - review & editing. **Jonathan Murnick**: Resources, Writing - review & editing. **Taeun Chang**: Conceptualization, Resources, Writing - review & editing. **Adre du Plessis**: Conceptualization, Writing - review & editing, Supervision. **Catherine Limperopoulos**: Conceptualization, Methodology, Writing - review & editing, Supervision, Project administration, Funding acquisition.

Appendix A. Supplementary data

Supplementary data to this article can be found online at https://doi.org/10.1016/j.neuroimage.2020.117043.

suggesting that extra-uterine environment exposure alters the development of select neural networks in the absence of structural brain injury.

Keywords

Functional connectivity; In utero versus ex utero brain function; Premature birth; Resting state MRI

1. Introduction

Preterm birth may influence critical steps of third trimester and early postnatal brain development, including neuronal migration, synaptogenesis, dendritic arborization, selective elimination of neuronal processes and synapses, and axonal myelination (Malik et al., 2013; Tau and Peterson, 2010; Tibrewal et al., 2018; Volpe et al., 2017). The precise impact of early exposure to the extra-uterine environment on neurodevelopmental outcomes (Blencowe et al., 2013) in children born premature has yet to be fully explored. However, recent studies using advanced brain imaging techniques have shown altered metabolic profiles (Ball et al., 2013a, 2013b; Basu et al., 2019; Kwon et al., 2014; Vinall et al., 2013), cortical surface changes (Ajayi-Obe et al., 2000; Boardman et al., 2007; Lefèvre et al., 2016; Orasanu et al., 2016), and impaired brain growth (Padilla et al., 2015) in prematurely born infants. Cerebral and cerebellar growth trajectories in third trimester preterm infants without brain injury also lagged behind healthy in utero fetuses (Bouyssi-Kobar et al., 2016).

Brain functional network organization has also been shown to be altered in infants born premature. Early studies using resting state functional connectivity MRI (rs-fcMRI), which allows simultaneous, noninvasive assessment of multiple brain networks, have shown some resting state networks in preterm brains that resemble adult architecture (Doria et al., 2010; Fransson et al., 2007). More recent studies between premature infants at term equivalent age and healthy full-term newborns have shown connectivity differences such as reduced magnitude of the blood oxygenation level dependent (BOLD) responses, reduced BOLD complexity, altered thalamocortical connectivity, and altered functional network segregation and integration in premature infants (Bouyssi-Kobar et al., 2019; Smyser et al., 2014; Toulmin et al., 2015). These investigations, along with others (Doria et al., 2010; Smyser et al., 2010) have provided critical insights into how the brain's functional connectivity changes over time in premature infants. However, in-vivo comparisons with healthy gestational age-matched control fetuses are needed to better understand impaired network organization due to premature exposure to the ex utero environment. Recently, rs-fcMRI has been successfully used to probe brain function in utero (Rutherford et al., 2019; Schöpf et al., 2012; Thomason et al., 2014, 2014a, 2013) describing robust bilateral connectivity between homologous structures in the fetal brain. Similar to the premature brain (Doria et al., 2010; Smyser et al., 2010), these interhemispheric connections display a medial to lateral connectivity gradient, with medial areas of the brain sharing stronger connections.

In the present study, we investigated functional connectivity in very premature infants (born at 32 weeks gestational age, GA, or earlier) and compared them to gestational age-matched healthy in-utero fetuses. Our goal was to characterize the effects of early exposure to the

extra-uterine environment on the developing third trimester brain networks that may serve as early markers of altered brain development in prematurity.

2. Methods

2.1. Participants

Infants born at ≤32 weeks GA admitted in the Neonatal Intensive Care Unit (NICU) at the Children's National Medical Center (CNMC, Washington, DC) were recruited to a longitudinal observational study investigating brain development in premature infants. Premature infants with cerebral or cerebellar parenchymal lesions, brain malformation, dysmorphic features or congenital anomalies suggestive of a genetic/chromosomal disorder, metabolic disorder, or congenital central nervous system infection were excluded. Anatomic MR images were reviewed and assessed as structurally normal (i.e. no parenchymal brain lesions/injury) by a pediatric neuroradiologist (J.M.). Fetuses with GAs matching the premature cohort were selected from a normative study that enrolled healthy pregnant women with normal fetal ultrasounds (Andescavage et al., 2017). Exclusion criteria included multiple pregnancies, chromosomal abnormalities, and congenital infection. Both studies were approved by the institutional review board of Children's National in Washington, DC and written informed consent was obtained from study participants.

2.2. MRI acquisition

Fetal and premature images were acquired using a 1.5T MRI scanner (GE Healthcare, Milwaukee, WI). Sagittal, axial, and coronal anatomical T2-weighted images were collected using a single-shot fast spin echo sequence with slice thickness of 2 mm. Gradient-echo planar images (EPI) in premature infants were acquired with the following parameters: repetition time (TR), 2000; echo time (TE), 30; median slice thickness, 4 mm; flip angle, 60°, median in-plane resolution, 2.34 × 2.34 × 4.00 mm and scan duration, 8.27 ± 1.70 min. In fetuses, the scan settings were: TR, 3000; TE, 60; median slice thickness, 3 mm; flip angle, 90°, median in-plane resolution, 2.5 × 2.5 × 3.00 mm and scan duration, 7.00 min. Premature MRIs were performed during natural sleep using a feed-and-swaddle technique; none of the premature infants were sedated during scan. Premature infants requiring temperature monitoring were scanned using a MRI-compatible incubator (LMT Medical Systems GmbH, Lue-beck, Germany).

2.3. Preprocessing of resting state data

Premature and fetal resting state data were preprocessed to minimize non-neural contributions (i.e., motion-related effects, cardiac and respiratory noise, and scanner-related drifts) to the BOLD signal (Caballero-Gaudes and Reynolds, 2017; Jo et al., 2013); the same denoising strategies were used for both cohorts. Slice timing correction was first performed followed by exclusion of the first four volumes of the time series to ensure steady-state longitudinal magnetization. EPI images were then oriented to radiologic convention using their corresponding GA template (Gholipour et al., 2014) as reference. Resting state data were then despiked and bias field-corrected (Tustison et al., 2010). At this point, volumes where more than 10% of voxels were considered signal intensity outliers based on how much each voxel's signal deviated from its BOLD time series trend were identified for later

censoring. The EPI images were then corrected for motion using a two-pass registration approach optimized for fetuses and infants to correct for large and small head movements (developed by DS) (Joshi et al., 2011; Scheinost et al., 2018). High motion volumes were then defined based on the head realignment parameters (i.e., rigid body transformations) from the previous motion correction step. Frames with translational motion >1 mm and rotational motion >1.5° were considered high motion; these cut-offs were based on thresholds used in recently published fetal resting state studies (Li et al., 2019; Thomason et al., 2019, 2017; van den Heuvel et al., 2018; Wheelock et al., 2019). Volumes with frame-to-frame motion (i.e., framewise displacement, FD) >1.5 mm were also excluded. These high motion frames were eventually 'scrubbed' or removed from the time series (described below) to further attenuate confounding effects of motion on functional connectivity. The EPI and anatomic images were then coregistered: to achieve better alignment, especially in fetal images, resting state data were first manually aligned (using AFNI's Nudge plug-in) (Cox, 1996) to the fetal/premature T2 brain followed by an automatic registration of the anatomic image to the EPI brain. During this step, white matter (WM) and cerebrospinal fluid (CSF) tissue segmentations defined in high-resolution anatomical images were also transformed to the EPI images; this allowed definition of WM and CSF tissues in the EPI data. The resting state data was then intensity scaled to a global mode of 1000 (Ojemann et al., 1997) followed by smoothing using an isotropic 5 mm full-width at half-maximum Gaussian kernel. Band-pass filtering (0.009 Hz–0.08 Hz) and nuisance regression were then performed simultaneously on the EPI-BOLD data (Behzadi et al., 2007; Hallquist et al., 2013). Regressors included tissue- and motion-derived signals. Signals from eroded and localized white matter (WM; AFNI's @ANATICOR(Jo et al., 2010)) and the first five principal components of the averaged cerebrospinal fluid (CSF) signal (Behzadi et al., 2007; Muschelli et al., 2014) comprised tissue-based regressors. Motion regressors included linearly detrended translational and rotational head motion parameters, their temporal derivatives, and quadratic terms (Friston et al., 1996; Worsley et al., 1996). Censoring of previously identified volumes was performed with regression to preserve temporal dependencies between signals. After regression, residual BOLD signals were analyzed in EPI space.

2.4. Analysis of rs-fcMRI data

The duration of premature scans was longer than fetal scans. In addition, the number of remaining volumes after preprocessing also tended to be greater in premature infants. To address this, we reduced the number of volumes analyzed in premature subjects so that the total scan duration between groups matched (see Supplementary Information).

Blood oxygenation level dependent (BOLD) signals were measured from 23 regions of interest (ROIs) per hemisphere (Fig. 1A) after intensity-based masking of label masks (Peer et al., 2016). ROIs were semi-automatically defined using the DrawEM segmentation software (Makropoulos et al., 2014). For each group, seed-based correlation analysis was performed to determine connectivity across all 46 seeds. The Pearson product-moment correlation between the BOLD time series of all possible ROIs pairs, a total of 1035 correlations, was computed. Pearson correlation coefficients (r) were Fisher-z transformed (r_z) then r_z scores for each ROI pair were evaluated for significance using t tests. To correct

for multiple comparisons across the whole brain, only connections with false discovery rate (FDR) adjusted p-value<0.05 were considered significant (Benjamini and Hochberg, 2000). Whole brain connectivity strength was then correlated with gender, GA/postmenstrual age (PMA), motion (i.e. framewise displacement), image smoothness (x, y, and z) and regional temporal signal to noise ratio (TSNR).

With regards to the latter two variables, differences in scanner settings can affect image spatial smoothness and TSNR (i.e., the average voxel signal divided by the temporal standard deviation of the voxel time series); increased smoothness enhances TSNR and this, in turn, may impact estimated BOLD activation (Friedman et al., 2006b, 2006a; Parrish et al., 2000). To evaluate the influence of varying smoothness and TSNR on functional connectivity, average smoothness of the residual images along the x, y, and z directions measured using AFNI's 3dFWHMx and gray matter TSNR at each ROI (i.e. regional TSNR) of motion corrected images prior to nuisance regression and censoring were computed for each group and correlated with functional connectivity across all ROI pairs. If connectivity strength was influenced by these factors, then these effects would manifest as, for example, increased connectivity with increased TSNR. It is worth noting that while increasing TSNR increases sensitivity to BOLD signal changes (Parrish et al., 2000), one study has demonstrated consistent resting state connectivity (i.e., default mode network) using seed-based correlation and independent component analyses despite TSNR differences (Jovicich et al., 2016; Parrish et al., 2000).

Functional connectivity differences between groups were estimated using network-based statistics (NBS) (Zalesky et al., 2010). NBS detects subnetworks – subsets of nodes and their connections – where connectivity strength differs significantly between groups. This technique allows greater power to detect between-group differences compared to mass univariate testing. NBS uses permutation testing to determine significance. Here, data were permuted 10,000 times, using a family-wise error (FWE) corrected p-value of $p < 0.05$, and using an initial t threshold of 2.1; this t statistic corresponds to a $p < 0.05$. Gender, GA/PMA, motion (i.e., framewise displacement) and smoothness along the x and z dimensions were included as covariates in the general linear model. Previous variance inflation factor (Akinwande et al., 2015; Robinson and Schumacker, 2009) assessment to diagnose multicollinearity among covariates identified smoothness along the y direction and regional TSNR as collinear with group assignment (i.e. healthy fetus vs. premature infant); these variables were thus excluded from the NBS regression. Removing co-linear variables allows the proper interpretation of standard errors of the coefficients of regression.

To determine whether connectivity displayed medial to lateral organization, we used a regression model relating connectivity strength between homologous pairs, r_z, and the ROIs distance from the midline of the brain. Distance was defined by identifying the medoid, the voxel with the minimal Euclidean distance from all other voxels in the ROI label mask. The x coordinate of the medoid defined a region's lateral position. To account for the increase in brain size with advancing gestational age and the dolicocephaly observed in some premature brains (McCarty et al., 2017), distances were normalized to the maximum distance for each brain (i.e., the distance of the most lateral ROI from the mid-sagittal plane). Linear and nonlinear models were evaluated and the best fitting model to describe the relationship

between connectivity and distance was identified by assessing adjusted R-square values and comparing model fits using analysis of variance (ANOVA)(Chambers and Hastie, 1992). All analyses were performed on r_Z scores but tables and figures show Pearson correlation coefficients for ease of interpretation. Data and results are reported as means ± standard deviation (SD), unless otherwise stated.

3. Results

3.1. Clinical characteristics of study participants

Fifty age-matched healthy fetuses (n = 25) and premature infants (n = 25) were included for this analysis. Premature infants were scanned between 26 and 33 weeks PMA (30.77 ± 2.14 weeks) and healthy fetuses between 26 and 34 weeks GA (30.77 ± 2.52 weeks). Table 1 summarizes the clinical characteristics of our study cohorts.

3.2. Quality assurance of resting state data

On average, we analyzed 5.31 min of data for each group (Table 2), representing 75.89% and 67.08% of collected data from fetuses and premature infants, respectively. All analyzed time series data were >4 min in duration.

Maximum and average frame-to-frame motion was significantly less in premature infants compared to fetuses ($p < 0.001$). Averaged maximum frame-to-frame translational and rotational displacement (i.e. averaged across x, y, and z directions) in fetuses was 0.57 mm and 0.99°, respectively; in premature infants, averaged maximum values were lower at 0.27 mm and 0.71°. Averaged mean frame-to-frame motion in fetuses was 0.13 mm and 0.20°, corresponding values in premature infants were 0.03 mm and 0.09°. Average and maximum framewise displacement values were also lower ($p < 0.001$) in premature infants compared to fetuses. Table 3 and the Supplemental Information provide additional details about head motion for the groups.

Spatial smoothness along the z-direction and TSNR (i.e., global and regional) were also significantly different between groups ($p < 0.001$).

3.3. Functional connectivity using seed based correlation analysis in healthy fetuses and premature infants

There were 327 (31.59% of 1035) significant connections involving all 46 nodes in premature infants (Fig. 1B). Average connectivity strength among significantly connected regions was 0.36 ± 0.13 (mean ± SD; range: 0.15–0.77). Among the significant edges, 182 out of 327 (55.66%) connected to ipsilateral regions, 142 to contralateral ROIs. Twenty crosshemispheric connections were shared between homologous areas (Fig. 1C); the three regions that were not strongly connected were the anterior to posterior medial and inferior temporal lobes and the posterior part of the fusiform gyrus. Connectivity strength in premature infants and fetuses did not correlate with age, gender, motion, image smoothness, and regional TSNR.

In healthy fetuses, there were 103 (9.95%) connections involving all 46 nodes (Fig. 1B). Average connectivity strength among significantly connected regions was 0.44 0.12 (mean ±

SD; range: 0.25–0.75). The majority of connections (84.47%) linked ipsilateral areas, a few connected contralateral regions. Of the latter, eight linked homologous pairs, namely the anterior and posterior cingulate, cerebellum, thalamus, frontal, parietal and occipital lobes, and lentiform nucleus (Fig. 1C). Similar to premature infants, we did not observe any correlation between connectivity strength and covariates.

The number of significant connections in fetuses was far less than in premature infants (two-proportion z test, $p < 0.05$). The proportion of ipsilateral versus contralateral edges differed significantly between groups (Fisher's exact test, $p < 0.05$). In premature infants, ipsilateral connections accounted for 55.66% (182/327) of significant links; in fetuses, the majority of links were ipsilateral (84.47%). Table 4 lists the top 20 strongest connections in both groups; see Table S1 and S2 for a complete list.

Fig. 2 shows statistical parametric maps showing resting connectivity patterns for some of the ROIs, specifically the left hippocampus, left cerebellum, and right anterior cingulate ($p < 0.001$). The hippocampal network was more localized and constrained to the ipsilateral hemisphere in fetuses while premature infants' maps extended to noncontiguous regions, including the contralateral medial temporal areas. Cerebellar networks were similarly robust in both groups, with strong L-R correlations seen in both cohorts. The ACC showed strong bilateral connectivity; the network extended to the dorsomedial prefrontal cortex and included areas of the deep gray matter and insula in the premature infants.

3.4. Comparison of functional brain networks using network-based statistics

Using NBS, we identified a single subnetwork ($p_{FWE} = 0.002$) comprised of 42 regions linked by 94 connections (94/1035 or 9% of all possible edges) where connectivity was greater in premature infants compared with healthy fetuses (Fig. 3). Between-group differences in connectivity strength were mostly observed in contralateral projections: 67.02% (63/94) of connections of the subnetwork connected left and right ROIs. Among these bilateral connections were those between homotopic regions of the brain, specifically the hippocampus, medial anterior temporal lobes, mid- to posterior superior temporal gyri, posterior middle and inferior temporal gyri, cerebella, insulae, occipital lobes, subthalamic and lentiform nuclei. In this subnetwork, the most involved nodes (i.e. high degree nodes) were bilateral mid- to posterior superior temporal gyrus, the right thalamus, and the left anterior cingulate gyrus. We did not observe subnetworks that were more strongly connected in fetuses compared with premature infants.

Although greater connectivity strength was observed between a number of ROIs in premature infants, the overall pattern of high to low connectivity (ranked according to Fisher-z transformed correlation values) were similar between groups ($r_{tau} = 0.30$, $p < 0.001$).

3.5. Medial to lateral connectivity gradient

Bilateral connectivity decreased in a curvilinear fashion from medial to lateral ROIs in both premature infants (quadratic model, adjusted R-square = 0.61, $p < 0.001$) and healthy fetuses (cubic model, adjusted R-square = 0.57, $p < 0.001$). The greater the distance the medoid of an ROI is from the middle plane of the brain, the weaker its connectivity to its contralateral

partner (Fig. 4). Connectivity between ROI pairs decreased more sharply in fetuses compared to premature infants.

4. Discussion

To the best of our knowledge, our study is the first to compare functional brain connectivity in premature infants without structural brain injury and age-matched healthy fetuses. Functional connectivity patterns between the two groups were similar, such that regions that were strongly linked in premature infants were likely to be strongly linked in fetuses; the same was true for weaker connections. However, some regional differences in functional connectivity strength were observed, notably involving medial temporal lobe regions, the basal ganglia, superior temporal gyri and occipital lobes. Differences in the number of significant ipsilateral versus cross-hemispheric connections were also noted. Our results suggest that early extra-uterine environment exposure alters the developmental trajectory of select neural networks in the absence of structural brain injury over the third trimester.

Our healthy fetal cohort showed robust bilateral connectivity in the cingulate, frontal cortex, basal ganglia (i.e. globus pallidus and putamen), cerebellum and occipital lobes, and lack of cross-hemispheric coactivity in the anterior and lateral temporal regions and insula. This connectivity pattern reflects the development of white matter bundles and progression of myelination in the nervous system. Myelination, specifically, proceeds in a cranio-caudad and central-to-peripheral direction and occurs earlier in visual and auditory regions compared to association areas (Brody et al., 1987; Kinney et al., 1988; Kostović et al., 2002). Our findings also corroborate previously reported fetal resting-state findings (Thomason et al., 2014, 2013). Thomason et al., reported that various areas within a lobe are differentially activated. For instance, while BOLD time series signals in bilateral premotor and orbitofrontal cortices were significantly correlated, those in the primary motor and somatosensory cortices were not. Unfortunately, the larger ROIs used in our study, defined using a segmentation method proven reliable across a wide range of gestational ages (Makropoulos et al., 2014), precluded such observations. Future studies that create finer parcellations of the cortices based on functional data (Craddock et al., 2012) could help clarify differential functional activation in the frontal, parietal and occipital cortices.

Previous studies in premature infants have shown significantly correlated cross-hemispheric activity in the cingulate, occipital, medial prefrontal, thalamic and cerebellar regions, among others; this is consistent with our findings at these ROIs in premature infants (Doria et al., 2010; Smyser et al., 2010). These studies have also demonstrated reduced connectivity strength in these areas in premature infants at term age compared to their healthy newborn counterparts. Interestingly in our younger cohorts (i.e., fMRI performed before term age), this relationship was reversed. The reasons for this are unclear, but in the visual system, for example, it is conceivable that healthy newborns, benefitting from optimal endogenous followed by well-timed activity-dependent stimulation (Graven, 2004), will have more mature cross-hemispheric connectivity during the postnatal period compared to infants whose immature visual systems were prematurely exposed to diverse visual stimuli (Madan et al., 2007). Reconciling these findings will require serial longitudinal MRI studies

following premature infants until term age and in utero fetuses that are born full-term. These important clinical studies are currently ongoing.

Our result of stronger connectivity between medial ROI pairs compared to lateral ones parallels findings from previous reports in fetuses and premature infants (Smyser et al., 2010). These studies have shown that connectivity in lateral areas of the brain increased as the brain matured (i.e. as premature infants' postnatal ages increase). The sharper decrease in connectivity noted in fetuses suggest that some functional networks may be more mature in premature infants, possibly because of environmental stimulation. Of note, medial ROIs, such as the frontal and parietal cortices, cingulate, and lentiform nucleus, etc., and medial temporal lobe structures that were strongly connected to their contralateral counterparts and to other brain regions have previously been reported as essential to global information processing in the adult brain and are called rich club hubs (van den Heuvel and Sporns, 2011). A study by Ball and colleagues (Ball et al., 2014) using diffusion tensor imaging in premature infants has shown that while some cortico-cortical and cortical-subcortical were disrupted in premature infants, rich club organization – where highly connected hubs are also highly connected to each other – involving brain areas that closely overlap strongly connected areas identified in this study was intact. In contrast, rich club organization in adults born VPT significantly differed from healthy controls (Karolis et al., 2016). Studies that longitudinally follow premature cohorts to assess how decreased connectivity strength during early brain development (i.e., ex-utero third trimester brain growth) between areas that are identified as critical for integrating information in the brain, such as the thalamus, lentiform, and hippocampus impact neurodevelopmental outcomes in premature infants would undoubtedly provide valuable insights.

Areas involved with sensory input, notably between the occipital lobes and superior temporal gyrus, showed stronger bilateral connectivity in the premature brain compared with the healthy fetal brain. Compared to in utero fetuses, the visual cortices in premature infants were more strongly connected (i.e., significant interhemispheric occipital connectivity). A previous study by our group has shown that premature infants at term age showed increased connection density in the occipital cortex compared to healthy newborns (Bouyssi-Kobar et al., 2019). This finding is also consistent with increased occipital cortex volumes reported by Padilla et al. (2015) in a cohort of extremely premature infants. Electrophysiologic and neurobehavioral studies also support accelerated visual system maturation in premature infants. Schwindt and colleagues reported decreased visual evoked potentials peak-times, indicating more mature visual cortex function, in 38 extremely premature infants; infants with greater postnatal ages also had faster times (Schwindt et al., 2018). Similarly, a study by Ricci et al. (2008) that compared eye tracking and ocular movements in term newborns and in very premature born infants at 35 and 40 weeks PMA also report an accelerated maturation process. In this study, very premature infants at 35 weeks showed less developed visual responses (i.e., following a black and white target) compared to 40 week premature infants; both groups, however, demonstrated more mature responses compared to healthy term newborns. Taken together, available converging evidence suggests accelerated visual network maturation in premature infants due to increased visual stimulation ex utero.

In our study, connectivity between the mid- to posterior portion of the superior temporal gyrus was also significantly greater in premature infants compared to fetuses. The posterior part of the superior temporal cortex is involved in hearing, language and speech; the auditory cortex (Heschl's gyrus) lies in the posterior part of this region (Howard et al., 2000). Similar to the occipital lobes, our findings perhaps reflect the effects of extrauterine auditory stimulation which are dampened in utero. Given the higher incidence of sensory modulation and processing abnormalities in premature infants, one wonders if premature stimulation of the visual and auditory cortices - especially considering the types of stimuli in the NICU (e.g., bright lights and high-frequency non-biological sounds) - adversely impacts development of these systems during this critical period (Bröring et al., 2017; Lahav and Skoe, 2014). Longitudinal studies in larger cohorts that investigate how connectivity in these areas in premature and healthy fetuses/infants evolves over time would help clarify the effects of early extra-uterine environment exposure to developing sensory systems.

Similar to sensory regions, areas involved with stress/pain pathways such as the hippocampus and insula showed robust bilateral connectivity in the premature brain compared to the healthy fetal brain. The hippocampus, along with the medial prefrontal cortex, controls the body's physiologic responses to stress (McEwen and Gianaros, 2010). We hypothesize that painful stimuli and exposure to postnatal stress during care in the NICU environment activates the limbic system, and accelerates formation of the observed connections (Maroney, 2003). Clinical studies suggest that early adverse stressful life experiences in premature infants alter neurobehavior later in life, possibly predisposing infants born premature to other psychopathologies such as depression and post-traumatic stress disorder (Chrousos, 2009). In rodents, one study showed that those exposed to a painful procedure on the first day of life had disrupted neural stress circuitry; specific areas affected included glucocorticoid receptors in the hippocampus, amygdala, and periaqueductal gray matter (Victoria et al., 2013a, Victoria et al., 2013). Long-term studies are needed to address this intriguing finding.

While we report atypical intra- and interhemispheric connectivity in premature infants during the early postnatal period, aberrant functional connectivity in premature infants during late infancy, school age, adolescence and adulthood involving ROIs related to those discussed have previously been reported (Gozzo et al., 2009; Rowlands et al., 2016; Scheinost et al., 2017; Smith et al., 2011; Toulmin et al., 2015). This suggests that neural circuitry changes that potentially underlie neurobehavioral impairments in premature infants begin as early as the third trimester of pregnancy, and possibly even earlier, and highlights the need for identifying these deviations early.

Despite the strength of being the first in vivo comparative study of neural network connectivity between premature infants and healthy fetuses prior to TEA, our study limitations deserve mention. First, scanning parameters used for premature infants and healthy fetuses were optimized to obtain the best possible images from participants and thus differed between cohorts. We, however, believe that the observed between-group differences are due to differences in physiology rather than differences in the acquisition parameters. If due to the latter, then we would expect to observe global increases or decreases in connectivity in one group compared to the other. For example, if signal to noise ratio was

lower in fetal scans leading to inability to detect some signals, then connectivity in fetuses, including in the frontal lobe, cingulate and cerebellum should also be depressed. Second, our cohort size is relatively small and studies on larger cohorts of infants covering a broader gestational age range would allow us to better characterize differences between the two groups and to relate neuroimaging findings to clinical variables. However, as the first study to explore functional connectivity in these two cohorts, our samples sizes are consistent with the literature (Doria et al., 2010; Smyser et al., 2010; Thomason et al., 2013). Third, our fetal cohort had significantly higher motion than our premature group. Studies have shown that while motion influences the dependence between connectivity and inter-ROI distance, connectivity differences persist after properly accounting for motion (Ciric et al., 2017; Power et al., 2015, 2012; Satterthwaite et al., 2013). Correcting for motion in the fetal cohort, however, is challenging. While we can minimize the effect of motion using different strategies, acquiring more low motion fetal data enabling motion-matched comparisons is our continuing goal. Lastly, although we included only infants with no evidence of parenchymal brain injury in our study, there could be smaller lesions that remain undetected because it is below the resolution limits of conventional MRI (Pierson et al., 2007).

5. Conclusion

Our data suggest that early extrauterine exposure alters functional brain connectivity in premature infants without structural brain injury. Neural circuitry reorganization in premature infants was observed in the sensory input areas including occipital and temporal regions; as well as stress and nociceptive pathways including the hippocampus. Additional studies that explore how altered connectivity relates to clinical risk factors of prematurity, brain volumetric growth and quantifiable measures of stress are necessary to clarify the impact of very premature birth on the developing brain.

Supplementary Material

Refer to Web version on PubMed Central for supplementary material.

Acknowledgments

Funding

This work was supported by the National Institutes of Health [NHLBI R01HL116585 and IDDRC U54HD090257] and the Canadian Institute of Health Research [MOP-81116].

References

Ajayi-Obe M, Saeed N, Cowan FM, Rutherford MA, Edwards AD, 2000 Reduced development of cerebral cortex in extremely preterm infants. Lancet 356, 1162–1163. [PubMed: 11030298]

Akinwande MO, Dikko HG, Samson A, 2015 Variance inflation factor: as a condition for the inclusion of suppressor variable(s) in regression analysis. Open J. Stat 5 (7), 754 10.4236/ojs.2015.57075.

Andescavage NN, du Plessis A, McCarter R, Serag A, Evangelou I, Vezina G, Robertson R, Limperopoulos C, 2017 Complex trajectories of brain development in the healthy human fetus. Cerebr. Cortex 27, 5274–5283.

Ball G, Aljabar P, Zebari S, Tusor N, Arichi T, Merchant N, Robinson EC, Ogundipe E, Rueckert D, Edwards AD, Counsell SJ, 2014 Rich-club organization of the newborn human brain. Proc. Natl. Acad. Sci. U.S.A 111, 7456–7461. [PubMed: 24799693]

Ball G, Boardman JP, Aljabar P, Pandit A, Arichi T, Merchant N, Rueckert D, Edwards AD, Counsell SJ, 2013a The influence of preterm birth on the developing thalamocortical connectome. Cortex 49, 1711–1721. [PubMed: 22959979]

Ball G, Srinivasan L, Aljabar P, Counsell SJ, Durighel G, Hajnal JV, Rutherford MA, Edwards AD, 2013b Development of cortical microstructure in the preterm human brain. Proc. Natl. Acad. Sci. U.S.A 110, 9541–9546. [PubMed: 23696665]

Basu SK, Pradhan S, Kapse K, McCarter R, Murnick J, Chang T, Limperopoulos C, 2019 Third trimester cerebellar metabolite concentrations are decreased in very premature infants with structural brain injury. Sci. Rep 9, 1212. [PubMed: 30718546]

Behzadi Y, Restom K, Liau J, Liu TT, 2007 A component based noise correction method (CompCor) for BOLD and perfusion based fMRI. Neuroimage 37, 90–101. [PubMed: 17560126]

Benjamini Y, Hochberg Y, 2000 On the adaptive control of the false discovery rate in multiple testing with independent statistics. J. Educ. Behav. Stat 25, 60–83.

Blencowe H, Lee ACC, Cousens S, Bahalim A, Narwal R, Zhong N, Chou D, Say L, Modi N, Katz J, Vos T, Marlow N, Lawn JE, 2013 Preterm birth–associated neurodevelopmental impairment estimates at regional and global levels for 2010. Pediatr. Res 74, 17. [PubMed: 24366461]

Boardman JP, Counsell SJ, Rueckert D, Hajnal JV, Bhatia KK, Srinivasan L, Kapellou O, Aljabar P, Dyet LE, Rutherford MA, Allsop JM, Edwards AD, 2007 Early growth in brain volume is preserved in the majority of preterm infants. Ann. Neurol 62, 185–192. [PubMed: 17696128]

Bouyssi-Kobar M, De Asis-Cruz J, Murnick J, 2019 Altered functional brain network integration, segregation, and modularity in infants born very preterm at term-equivalent age. The Journal of 213, 13–21.

Bouyssi-Kobar M, du Plessis AJ, McCarter R, Brossard-Racine M, Murnick J, Tinkleman L, Robertson RL, Limperopoulos C, 2016 Third trimester brain growth in preterm infants compared with in utero healthy fetuses. Pediatrics 138 10.1542/peds.2016-1640.

Brody BA, Kinney HC, Kloman AS, Gilles FH, 1987 Sequence of central nervous system myelination in human infancy. I. An autopsy study of myelination. J. Neuropathol. Exp. Neurol 46, 283–301. [PubMed: 3559630]

Bröring T, Oostrom KJ, Lafeber HN, Jansma EP, Oosterlaan J, 2017 Sensory modulation in preterm children: theoretical perspective and systematic review. PloS One 12 e0170828. [PubMed: 28182680]

Caballero-Gaudes C, Reynolds RC, 2017 Methods for cleaning the BOLD fMRI signal. Neuroimage 154, 128–149. [PubMed: 27956209]

Chambers JM, Hastie TJ, 1992 Linear Models. Chapter 4 of Statistical Models in S. Wadsworth & Brooks/Cole.

Chrousos GP, 2009 Stress and disorders of the stress system. Nat. Rev. Endocrinol 5, 374–381. [PubMed: 19488073]

Ciric R, Wolf DH, Power JD, Roalf DR, Baum GL, Ruparel K, Shinohara RT, Elliott MA, Eickhoff SB, Davatzikos C, Gur RC, Gur RE, Bassett DS, Satterthwaite TD, 2017 Benchmarking of participant-level confound regression strategies for the control of motion artifact in studies of functional connectivity. Neuroimage 154, 174–187. [PubMed: 28302591]

Cox RW, 1996 AFNI: software for analysis and visualization of functional magnetic resonance neuroimages. Comput. Biomed. Res 29, 162–173. [PubMed: 8812068]

Craddock RC, James GA, Holtzheimer PE, Hu XP, Mayberg HS, 2012 A whole brain fMRI atlas generated via spatially constrained spectral clustering. Hum. Brain Mapp 33, 1914–1928. [PubMed: 21769991]

Doria V, Beckmann CF, Arichi T, Merchant N, Groppo M, Turkheimer FE, Counsell SJ, Murgasova M, Aljabar P, Nunes RG, Larkman DJ, Rees G, Edwards AD, 2010 Emergence of resting state networks in the preterm human brain. Proc. Natl. Acad. Sci. U.S.A 107, 20015–20020. [PubMed: 21041625]

Fransson P, Skiöld B, Horsch S, Nordell A, Blennow M, Lagercrantz H, Aden U, 2007 Resting-state networks in the infant brain. Proc. Natl. Acad. Sci. U.S.A 104, 15531–15536. [PubMed: 17878310]

Friedman L, Glover GH, Krenz D, Magnotta V, FIRST, B.I.R.N., 2006 Reducing interscanner variability of activation in a multicenter fMRI study: role of smoothness equalization. Neuroimage 32, 1656–1668. [PubMed: 16875843]

Friedman L, Glover GH, The FBIRN Consortium, 2006 Reducing interscanner variability of activation in a multicenter fMRI study: controlling for signal-to-fluctuation-noise-ratio (SFNR) differences. Neuroimage 33 (2), 471–481. 10.1016/j.neuroimage.2006.07.012.

Friston KJ, Williams S, Howard R, Frackowiak RSJ, Turner R, 1996 Movement-related effects in fMRI time-series. Magn. Reson. Med 35, 346–355. [PubMed: 8699946]

Gholipour A, Limperopoulos C, Clancy S, Clouchoux C, Akhondi-Asl A, Estroff JA, Warfield SK, 2014 Construction of a deformable spatiotemporal MRI atlas of the fetal brain: evaluation of similarity metrics and deformation models In: Medical Image Computing and Computer-Assisted Intervention – MICCAI 2014, Lecture Notes in Computer Science. Springer International Publishing, pp. 292–299.

Gozzo Y, Vohr B, Lacadie C, Hampson M, Katz KH, Maller-Kesselman J, Schneider KC, Peterson BS, Rajeevan N, Makuch RW, Constable RT, Ment LR, 2009 Alterations in neural connectivity in preterm children at school age. Neuroimage 48, 458–463. [PubMed: 19560547]

Graven SN, 2004 Early neurosensory visual development of the fetus and newborn. Clin. Perinatol 31, 199–216 v. [PubMed: 15289028]

Hallquist MN, Hwang K, Luna B, 2013 The nuisance of nuisance regression: spectral misspecification in a common approach to resting-state fMRI preprocessing reintroduces noise and obscures functional connectivity. Neuroimage 82, 208–225. [PubMed: 23747457]

Howard MA, Volkov IO, Mirsky R, Garell PC, Noh MD, Granner M, Damasio H, Steinschneider M, Reale RA, Hind JE, Brugge JF, 2000 Auditory cortex on the human posterior superior temporal gyrus. J. Comp. Neurol 416, 79–92. [PubMed: 10578103]

Jo HJ, Gotts SJ, Reynolds RC, Bandettini PA, Martin A, Cox RW, Saad ZS, 2013 Effective preprocessing procedures virtually eliminate distance-dependent motion artifacts in resting state FMRI. J. Appl. Math, 935154 10.1155/2013/935154, 2013.

Jo HJ, Saad ZS, Simmons WK, Milbury LA, Cox RW, 2010 Mapping sources of correlation in resting state FMRI, with artifact detection and removal. Neuroimage 52, 571–582. [PubMed: 20420926]

Joshi A, Scheinost D, Okuda H, Belhachemi D, Murphy I, Staib LH, Papademetris X, 2011 Unified framework for development, deployment and robust testing of neuroimaging algorithms. Neuroinformatics 9, 69–84. [PubMed: 21249532]

Jovicich J, Minati L, Marizzoni M, Marchitelli R, Sala-Llonch R, Bartrés-Faz D, Arnold J, Benninghoff J, Fiedler U, Roccatagliata L, Picco A, Nobili F, Blin O, Bombois S, Lopes R, Bordet R, Sein J, Ranjeva J-P, Didic M, Gros-Dagnac H, Payoux P, Zoccatelli G, Alessandrini F, Beltramello A, Bargalló N, Ferretti A, Caulo M, Aiello M, Cavaliere C, Soricelli A, Parnetti L, Tarducci R, Floridi P, Tsolaki M, Constantinidis M, Drevelegas A, Rossini PM, Marra C, Schönknecht P, Hensch T, Hoffmann K-T, Kuijer JP, Visser PJ, Barkhof F, Frisoni GB, Consortium, PharmaCog, 2016 Longitudinal reproducibility of default-mode network connectivity in healthy elderly participants: a multicentric resting-state fMRI study. Neuroimage 124, 442–454. [PubMed: 26163799]

Karolis VR, Froudist-Walsh S, Brittain PJ, Kroll J, Ball G, Edwards AD, Dell'Acqua F, Williams SC, Murray RM, Nosarti C, 2016 Reinforcement of the brain's rich-club architecture following early neurodevelopmental disruption caused by very preterm birth. Cerebr. Cortex 26, 1322–1335.

Kinney HC, Brody BA, Kloman AS, Gilles FH, 1988 Sequence of central nervous system myelination in human infancy. II. Patterns of myelination in autopsied infants. J. Neuropathol. Exp. Neurol 47, 217–234. [PubMed: 3367155]

Kostović I, Judaš M, Radoš M, Hrabač P, 2002 Laminar organization of the human fetal cerebrum revealed by histochemical markers and magnetic resonance imaging. Cerebr. Cortex 12, 536–544.

Kwon SH, Scheinost D, Lacadie C, Benjamin J, Myers EH, Qiu M, Schneider KC, Rothman DL, Constable RT, Ment LR, 2014 GABA, resting-state connectivity and the developing brain. Neonatology 106, 149–155. [PubMed: 24970028]

Lahav A, Skoe E, 2014 An acoustic gap between the NICU and womb: a potential risk for compromised neuroplasticity of the auditory system in preterm infants. Front. Neurosci 8, 381. [PubMed: 25538543]

Lefèvre J, Germanaud D, Dubois J, Rousseau F, de Macedo Santos I, Angleys H, Mangin J-F, Hüppi PS, Girard N, De Guio F, 2016 Are developmental trajectories of cortical folding comparable between cross-sectional datasets of fetuses and preterm newborns? Cerebr. Cortex 26, 3023–3035.

Li X, Hect J, Thomason M, Zhu D, 2019 Interpreting Age Effects of Human Fetal Brain from Spontaneous fMRI Using Deep 3D Convolutional Neural Networks arXiv [eess.IV]

Madan A, Jan JE, Good WV, 2007 Visual development in preterm infants. Dev. Med. Child Neurol 47, 276–280.

Makropoulos A, Gousias IS, Ledig C, Aljabar P, Serag A, Hajnal JV, Edwards AD, Counsell SJ, Rueckert D, 2014 Automatic whole brain MRI segmentation of the developing neonatal brain. IEEE Trans. Med. Imag 33, 1818–1831.

Malik S, Vinukonda G, Vose LR, Diamond D, Bhimavarapu BBR, Hu F, Zia MT, Hevner R, Zecevic N, Ballabh P, 2013 Neurogenesis continues in the third trimester of pregnancy and is suppressed by premature birth. J. Neurosci 33, 411–423. [PubMed: 23303921]

Maroney DI, 2003 Recognizing the potential effect of stress and trauma on premature infants in the NICU: how are outcomes affected? J. Perinatol 23, 679–683. [PubMed: 14647168]

McCarty DB, Peat JR, Malcolm WF, Smith PB, Fisher K, Goldstein RF, 2017 Dolichocephaly in preterm infants: prevalence, risk factors, and early motor outcomes. Am. J. Perinatol 34, 372–378. [PubMed: 27588933]

McEwen BS, Gianaros PJ, 2010 Central role of the brain in stress and adaptation: links to socioeconomic status, health, and disease. Ann. N. Y. Acad. Sci 1186, 190–222. [PubMed: 20201874]

Muschelli J, Nebel MB, Caffo BS, Barber AD, Pekar JJ, Mostofsky SH, 2014 Reduction of motion-related artifacts in resting state fMRI using aCompCor. Neuroimage 96, 22–35. [PubMed: 24657780]

Ojemann JG, Akbudak E, Snyder AZ, McKinstry RC, Raichle ME, Conturo TE, 1997 Anatomic localization and quantitative analysis of gradient refocused echo-planar fMRI susceptibility artifacts. Neuroimage 6, 156–167. [PubMed: 9344820]

Orasanu E, Melbourne A, Cardoso MJ, Lomabert H, Kendall GS, Robertson NJ, Marlow N, Ourselin S, 2016 Cortical folding of the preterm brain: a longitudinal analysis of extremely preterm born neonates using spectral matching. Brain Behav 6 e00488. [PubMed: 27257515]

Padilla N, Alexandrou G, Blennow M, Lagercrantz H, Ådén U, 2015 Brain growth gains and losses in extremely preterm infants at term. Cerebr. Cortex 25, 1897–1905.

Parrish TB, Gitelman DR, LaBar KS, Mesulam M-M, 2000 Impact of signal-to-noise on functional MRI. Magn. Reson. Med.: Off. J.Int.Soc.Magn. Reson. Med 44, 925–932.

Peer M, Abboud S, Hertz U, Amedi A, Arzy S, 2016 Intensity-based masking: a tool to improve functional connectivity results of resting-state fMRI. Hum. Brain Mapp 37 (7), 2407–2418. 10.1002/hbm.23182. [PubMed: 27018565]

Pierson CR, Folkerth RD, Billiards SS, Trachtenberg FL, Drinkwater ME, Volpe JJ, Kinney HC, 2007 Gray matter injury associated with periventricular leukomalacia in the premature infant. Acta Neuropathol 114, 619–631. [PubMed: 17912538]

Power JD, Barnes KA, Snyder AZ, Schlaggar BL, Petersen SE, 2012 Spurious but systematic correlations in functional connectivity MRI networks arise from subject motion. Neuroimage 59, 2142–2154. [PubMed: 22019881]

Power JD, Schlaggar BL, Petersen SE, 2015 Recent progress and outstanding issues in motion correction in resting state fMRI. Neuroimage 105, 536–551. [PubMed: 25462692]

Ricci D, Cesarini L, Romeo DMM, Gallini F, Serrao F, Groppo M, De Carli A, Cota F, Lepore D, Molle F, Ratiglia R, De Carolis MP, Mosca F, Romagnoli C, Guzzetta F, Cowan F, Ramenghi LA,

Mercuri E, 2008 Visual function at 35 and 40 weeks' postmenstrual age in low-risk preterm infants. Pediatrics 122, e1193–e1198. [PubMed: 19047222]

Robinson C, Schumacker RE, 2009 Interaction effects: centering, variance inflation factor, and interpretation issues. Multiple linear regression viewpoints 35, 6–11.

Rowlands MA, Scheinost D, Lacadie C, Vohr B, Li F, Schneider KC, Todd Constable R, Ment LR, 2016 Language at rest: a longitudinal study of intrinsic functional connectivity in preterm children. Neuroimage Clin 11, 149–157. [PubMed: 26937383]

Rutherford S, Sturmfels P, Angstadt M, Hect J, Wiens J, van den Heuvel MI, Scheinost D, Thomason M, Sripada C, 2019 Observing the origins of human brain development: automated processing of fetal fMRI. bioRxiv 10.1101/525386.

Satterthwaite TD, Wolf DH, Ruparel K, Erus G, Elliott MA, Eickhoff SB, Gennatas ED, Jackson C, Prabhakaran K, Smith A, Hakonarson H, Verma R, Davatzikos C, Gur RE, Gur RC, 2013 Heterogeneous impact of motion on fundamental patterns of developmental changes in functional connectivity during youth. Neuroimage 83, 45–57. [PubMed: 23792981]

Scheinost D, Onofrey JA, Kwon SH, Cross SN, Sze G, Ment LR, Papademetris X, 2018 A fetal fMRI specific motion correction algorithm using 2nd order edge features. In: 2018 IEEE 15th International Symposium on Biomedical Imaging (ISBI 2018) Ieeexplore ieee.org, pp. 1288–1292.

Scheinost D, Sinha R, Cross SN, Kwon SH, Sze G, Constable RT, Ment LR, 2017 Does prenatal stress alter the developing connectome? Pediatr. Res 81, 214–226. [PubMed: 27673421]

Schöpf V, Kasprian G, Brugger PC, Prayer D, 2012 Watching the fetal brain at "rest. Int. J. Dev. Neurosci 30, 11–17. [PubMed: 22044604]

Schwindt E, Giordano V, Rona Z, Czaba-Hnizdo C, Olischar M, Waldhoer T, Werther T, Fuiko R, Berger A, Klebermass-Schrehof K, 2018 The impact of extrauterine life on visual maturation in extremely preterm born infants. Pediatr. Res 84, 403–410. [PubMed: 29967524]

Smith GC, Gutovich J, Smyser C, Pineda R, Newnham C, Tjoeng TH, Vavasseur C, Wallendorf M, Neil J, Inder T, 2011 Neonatal intensive care unit stress is associated with brain development in preterm infants. Ann. Neurol 70, 541–549. [PubMed: 21976396]

Smyser CD, Inder TE, Shimony JS, Hill JE, Degnan AJ, Snyder AZ, Neil JJ, 2010 Longitudinal analysis of neural network development in preterm infants. Cerebr. Cortex 20, 2852–2862.

Smyser CD, Snyder AZ, Shimony JS, Mitra A, Inder TE, Neil JJ, 2014 Resting-state network complexity and magnitude are reduced in prematurely born infants. Cereb 26 (1), 322–333. 10.1093/cercor/bhu251. Cortex.

Tau GZ, Peterson BS, 2010 Normal development of brain circuits. Neuropsychopharmacology 35, 147–168. [PubMed: 19794405]

Thomason ME, Brown JA, Dassanayake MT, Shastri R, Marusak HA, Hernandez-Andrade E, Yeo L, Mody S, Berman S, Hassan SS, Romero R, 2014a Intrinsic functional brain architecture derived from graph theoretical analysis in the human fetus. PloS One 9 e94423. [PubMed: 24788455]

Thomason ME, Dassanayake MT, Shen S, Katkuri Y, Alexis M, Anderson AL, Yeo L, Mody S, Hernandez-Andrade E, Hassan SS, Studholme C, Jeong J-W, Romero R, 2013 Cross-hemispheric functional connectivity in the human fetal brain. Sci. Transl. Med 5, 173ra24.

Thomason ME, Grove LE, Lozon TA Jr., Vila AM, Ye Y, Nye MJ, Manning JH, Pappas A, Hernandez-Andrade E, Yeo L, Mody S, Berman S, Hassan SS, Romero R, 2014b Age-related increases in long-range connectivity in fetal functional neural connectivity networks in utero. Dev. Cogn. Neurosci 11, 96–104. 10.1016/j.dcn.2014.09.001. [PubMed: 25284273]

Thomason ME, Hect JL, Rauh VA, Trentacosta C, Wheelock MD, Eggebrecht AT, Espinoza-Heredia C, Burt SA, 2019 Prenatal lead exposure impacts cross-hemispheric and long-range connectivity in the human fetal brain. Neuroimage 191, 186–192. [PubMed: 30739062]

Thomason ME, Scheinost D, Manning JH, Grove LE, Hect J, Marshall N, Hernandez-Andrade E, Berman S, Pappas A, Yeo L, Hassan SS, Constable RT, Ment LR, Romero R, 2017 Weak functional connectivity in the human fetal brain prior to preterm birth. Sci. Rep 7, 39286. [PubMed: 28067865]

Tibrewal M, Cheng B, Dohare P, Hu F, Mehdizadeh R, Wang P, Zheng D, Ungvari Z, Ballabh P, 2018 Disruption of interneuron neurogenesis in premature newborns and reversal with estrogen treatment. J. Neurosci 38, 1100–1113. [PubMed: 29246927]

Toulmin H, Beckmann CF, O'Muircheartaigh J, Ball G, Nongena P, Makropoulos A, Ederies A, Counsell SJ, Kennea N, Arichi T, Tusor N, Rutherford MA, Azzopardi D, Gonzalez-Cinca N, Hajnal JV, Edwards AD, 2015 Specialization and integration of functional thalamocortical connectivity in the human infant. Proc. Natl. Acad. Sci. U.S.A 112, 6485–6490. [PubMed: 25941391]

Tustison NJ, Avants BB, Cook PA, Zheng Y, Egan A, Yushkevich PA, Gee JC, 2010 N4ITK: improved N3 bias correction. IEEE Trans. Med. Imag 29, 1310–1320.

van den Heuvel MI, Turk E, Manning JH, Hect J, Hernandez-Andrade E, Hassan SS, Romero R, van den Heuvel MP, Thomason ME, 2018 Hubs in the human fetal brain network. Dev. Cogn. Neurosci 30, 108–115. [PubMed: 29448128]

van den Heuvel MP, Sporns O, 2011 Rich-club organization of the human connectome. J. Neurosci 31, 15775–15786. [PubMed: 22049421]

Victoria NC, Inoue K, Young LJ, Murphy AZ, 2013a A single neonatal injury induces life-long deficits in response to stress. Dev. Neurosci 10.1159/000351121.

Victoria NC, Inoue K, Young LJ, Murphy AZ, 2013b Long-term dysregulation of brain corticotrophin and glucocorticoid receptors and stress reactivity by single early-life pain experience in male and female rats. Psychoneuroendocrinology 38 (12), 3015–3028. [PubMed: 24094874]

Vinall J, Grunau RE, Brant R, Chau V, Poskitt KJ, Synnes AR, Miller SP, 2013 Slower postnatal growth is associated with delayed cerebral cortical maturation in preterm newborns. Sci. Transl. Med 5, 168ra8.

Volpe JJ, Inder TE, Darras BT, de Vries LS, du Plessis AJ, Neil J, Perlman JM, 2017 Volpe's Neurology of the Newborn E-Book. Elsevier Health Sciences.

Wheelock MD, Hect JL, Hernandez-Andrade E, Hassan SS, Romero R, Eggebrecht AT, Thomason ME, 2019 Sex differences in functional connectivity during fetal brain development. Dev. Cogn. Neurosci 36, 100632. [PubMed: 30901622]

Worsley KJ, Marrett S, Neelin P, Vandal AC, Friston KJ, Evans AC, 1996 A unified statistical approach for determining significant signals in images of cerebral activation. Hum. Brain Mapp 4, 58–73. [PubMed: 20408186]

Zalesky A, Fornito A, Bullmore ET, 2010 Network-based statistic: identifying differences in brain networks. Neuroimage 53, 1197–1207. [PubMed: 20600983]

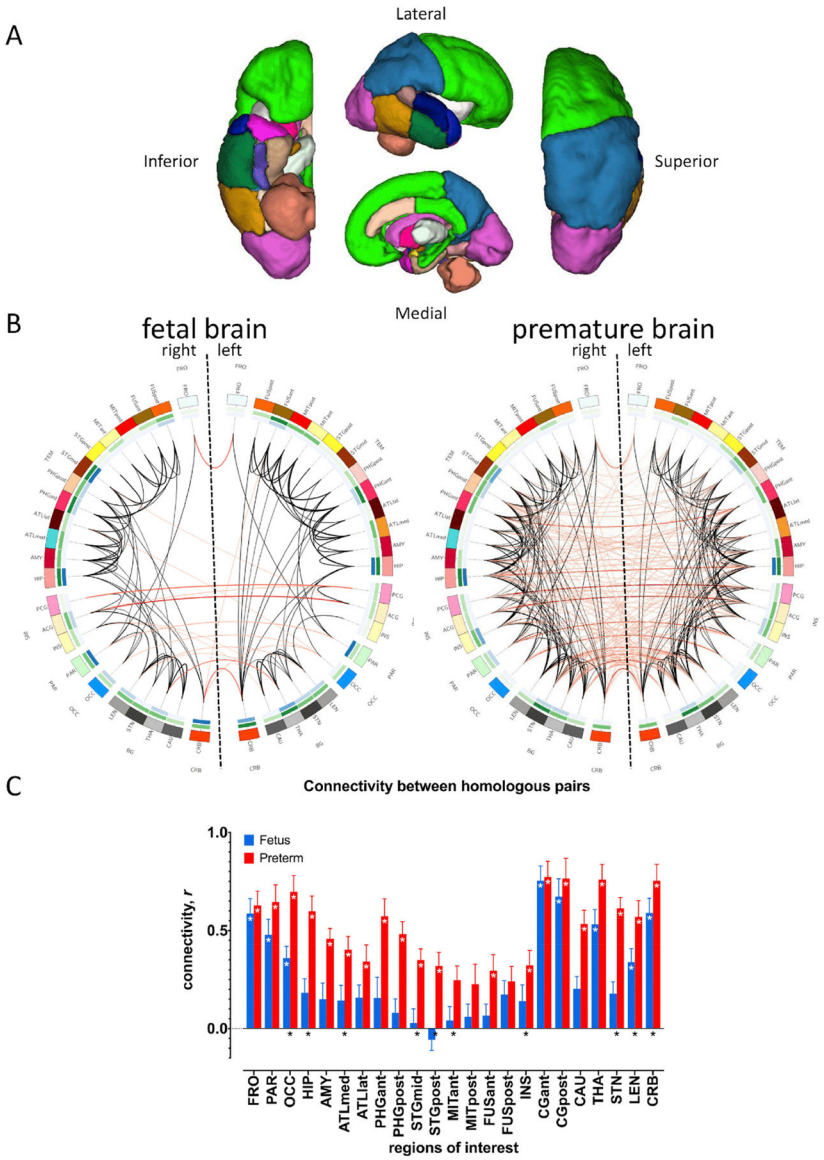

Fig. 1. Functional connectivity in fetuses and premature infants.

46 regions of interest (ROIs) are shown in (A). (B) shows whole brain connectivity in fetuses (left) and premature infants (right). Note greater number of significant and cross-hemispheric connections (red lines) in the latter; black lines – ipsilateral connections; darker lines indicate greater connectivity strength. Outermost circle shows 46 ROIs, middle green circle shows nodal degree (number of other regions connected to an ROI, darker hues indicate higher degree), innermost blue circle shows nodal betweenness (number of connections that pass through an ROI, again, darker colors mean higher betweenness). Cross-hemispheric connectivity between homologous ROI pairs shown in (C). Connections between 20/23 R-L ROI pairs significant in premature infants (red bars), marked by white asterisks; eight pairs were significant in fetuses (white asterisks); bilateral connections that were part of subnetwork with greater connectivity in premature infants marked by black asterisks at the bottom of the bars. White asterisks (*) = adjusted p_{FDR}<0.05; error bars

indicate standard error of the mean. Regions of interest: FRO, frontal; PAR, parietal; OCC, occipital; HIP, hippocampus; AMY, amygdala; ATLmed, anterior temporal lobe, medial part; ATLlat, anterior temporal lobe, lateral part; PHGant, gyri parahippocampalis et ambiens anterior part; PHGpost, gyri parahippocampalis et ambiens posterior part; STGmid, superior temporal gyrus, middle part; STp, superior temporal gyrus, posterior part; MITant, medial and inferior temporal gyri anterior part; MITpost, medial and inferior temporal gyri posterior part, FUSant, lateral occipitotemporal gyrus, gyrus fusiformis anterior part; FUSpost, lateral occipitotemporal gyrus, gyrus fusiformis posterior; INS, insula; CGant, cingulate gyrus, anterior part; CGpost, cingulate gyrus, posterior part; CAU, caudate; THA, thalamus; STN, subthalamic nucleus; LEN, lentiform nucleus; and, CRB, cerebellum.

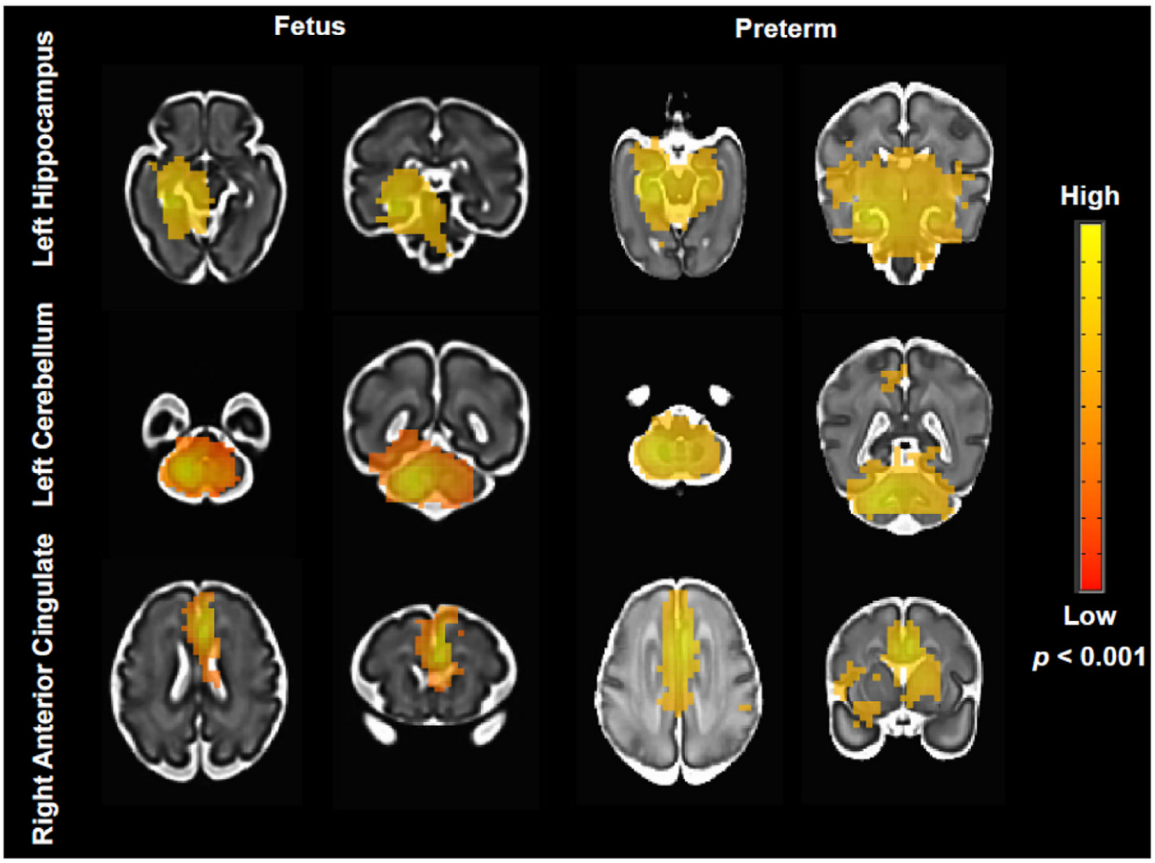

Fig. 2.

Averaged connectivity maps in representative ROIs: left hippocampus (top), left cerebellum (middle), and right anterior cingulate (bottom). Images are *t* statistical maps overlaid on high-resolution cohort-specific templates. Maps thresholded at $p < 0.001$ followed by AFNI's ClustSim; red to yellow indicate low to high *t* values.

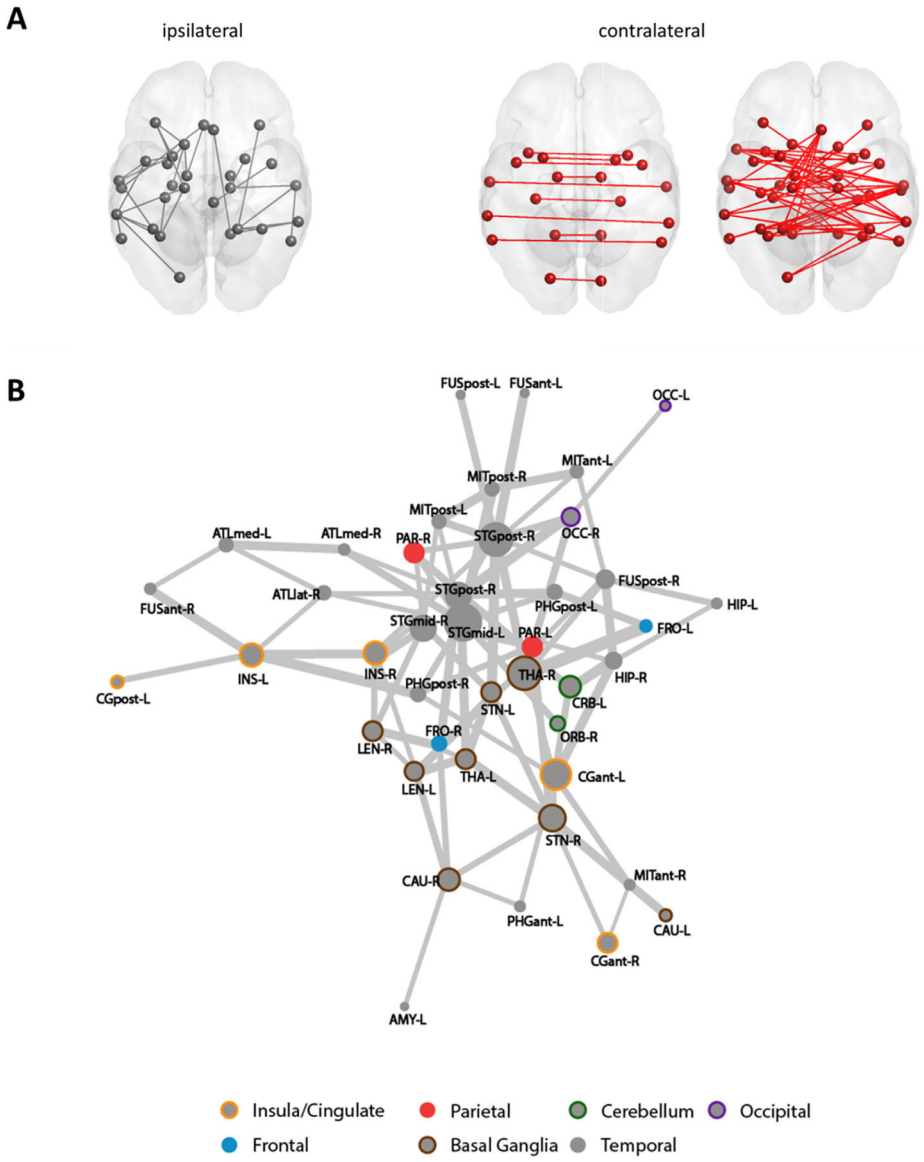

Fig. 3. Subnetwork with increased connectivity in premature infants compared to fetuses.

(A) shows ipsilateral (gray) and cross-hemispheric (red) connections that were different between groups. Force-directed graph (B) shows full subnetwork; line thickness reflect strength of differences; size of circle indicate number of other regions linked to an ROI; and, colors specify anatomical groupings based on Makropoulos (Makropoulos et al., 2014).

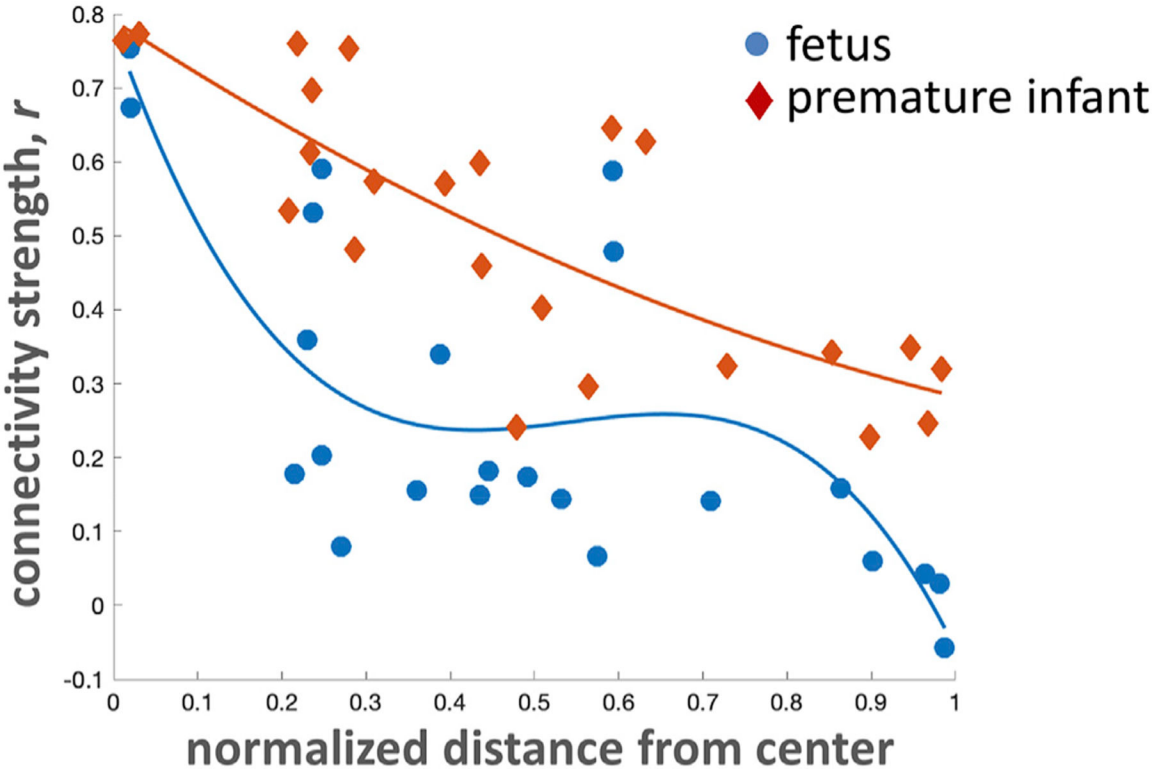

Fig. 4. Medial to lateral connectivity gradient.

Medial structures share stronger connections than lateral ones.

Table 1

Clinical characteristics of preterm infants and fetuses.

Clinical Characteristics	[1]Preterm	[2]Fetus	*p*
	n = 25	n = 25	
GA/PMA at MRI, wk	30.78 ± 2.14	30.77 ± 2.52	0.90
	26.14–33.57	26.71–34.29	
Day of life at MRI	16.84 ± 9.36	–	–
Female	16 (64)	12 (48)	
GA at birth, wk	28.37 ± 1.91	39.02 ± 1.06	***
	24.29–32.14	37–40.71	
Birth weight, g	1155.88 ± 307.43	3415.78 ± 476.32	***
	640–1995	2268–4265	
Small for GA	0 (0)	1 (4)	0.49
Vaginal delivery	8 (32)	13(59)	0.08
APGAR score at 5 min, median (range)	8 (2–9)	9 (6–9)	***
Highest level of ventilatory support			
High frequency ventilation	1 (4)		
Conventional ventilation	17 (68)		
NIPPV, Vapotherm or CPAP	5 (20)		
Minimum pH	7.32 ± 0.05		
Maximum pCO2, mmHg	45.84 ± 17.58		
Length of mechanical ventilation, d	14.88 ± 17.58		
	1–77		
Pressor support	3 (12)		
PDA	5 (20)		
PDA requiring ligation	1 (4)		
NEC	10 (40)		
NEC requiring surgery	2 (8)		
BPD	6 (24)		
Clinical infection	1 (4)		

Significance:

* < 0.05,

** < 0.01,

*** < 0.001;

data presented as mean ± SD (range) or n (% of n), unless specified otherwise. Gender, mode of delivery and SGA compared using Fisher's exact test; the rest compared using Mann-Whitney *U* Test.;

[1]APGAR score, minimum pH and maximum PCO_2 data from 24 premature infants, minimum PO_2 from 19 premature infants;

[2]Birth weight data from 23 fetuses, GA from 24, mode of delivery from 22, APGAR from 20; NIPPV – nasal intermittent positive pressure ventilation; CPAP – continuous positive airway pressure, PDA – patent ductus arteriosus, NEC – necrotizing enterocolitis, BPD – bronchopulmonary dysplasia.

Table 2

Duration of resting state scans (in minutes).

	Fetus		Premature infants		
	Mean	**SD**	**Mean**	**SD**	***p***
Scan duration	7	0	8.27	1.70	**
Retained after preprocessing (min, %)	5.41 (77.29)	0.64 (9.15)	7.50 (91.06)	1.82 (11.79)	***
Minimum scan length	4.40	–	4.13	–	
Maximum scan length	6.85	–	9.87	–	–
Retained for analysis (min, %)	5.31 (75.89)	0.64 (8.62)	5.31 (67.08)	0.63 (16.23)	0.70

Significance:

* < 0.05,

** < 0.01,

*** < 0.001.

Table 3

Summary of frame-by-frame motion in healthy fetuses and premature infants.

Metric	Fetus		Premature infants	
	Mean	SD	Mean	SD
Max excursion *x* (mm)	0.49	0.13	0.14	0.09
Max excursion *y* (mm)	0.53	0.19	0.25	0.12
Max excursion *z* (mm)	0.69	0.16	0.41	0.22
Max excursion pitch (°)	0.97	0.30	0.93	0.44
Max excursion yaw (°)	0.99	0.31	0.53	0.34
Max excursion roll (°)	1.01	0.24	0.67	0.50
Mean excursion *x* (mm)	0.11	0.03	0.01	0.01
Mean excursion *y* (mm)	0.12	0.05	0.03	0.02
Mean excursion *z* (mm)	0.17	0.06	0.04	0.03
Mean excursion pitch (°)	0.20	0.06	0.12	0.02
Mean excursion yaw (°)	0.20	0.06	0.06	0.04
Mean excursion roll (°)	0.20	0.05	0.07	0.06
RMS_{rel} *x* (mm)	0.14	0.04	0.03	0.02
RMS_{rel} *y* (mm)	0.17	0.06	0.06	0.03
RMS_{rel} *z* (mm)	0.23	0.07	0.03	0.05
RMS_{rel} pitch (°)	0.27	0.08	0.20	0.11
RMS_{rel} yaw (°)	0.27	0.08	0.10	0.06
RMS_{rel} *x* roll (°)	0.28	0.06	0.12	0.10
Max FD (mm)	1.32	0.17	0.74	0.34
Ave FD (mm)	0.48	0.11	0.12	0.08

Motion parameters are different between groups ($p < 0.01$) except for max excursion pitch (°).

Table 4

Top 20 significantly connected ROI pairs in fetuses and premature infants.

	Fetus			Premature infant		
	ROI 1	**ROI 1**	***r***	**ROI 1**	**ROI 1**	***r***
1	CGant-R	CGant-L	0.75	CGant-R	CGant-L	0.77
2	PHGant-L	FUSant-L	0.74	CGpost-R	CGpost-L	0.76
3	PHGant-R	FUSant-R	0.69	THA-R	THA-L	0.75
4	CGpost-R	CGpost-L	0.67	CAU-L	LEN-L	0.75
5	MITant-L	FUSant-L	0.66	CRB-L	CRB-R	0.75
6	ATLmed-L	PHGant-L	0.65	HIP-L	PHGant-L	0.70
7	AMY-R	ATLmed-R	0.63	OCC-R	OCC-L	0.70
8	ATLmed-R	ATLlat-R	0.62	CAU-R	LEN-R	0.69
9	CAU-R	LEN-R	0.61	HIP-R	PHGant-R	0.68
10	MITant-R	FUSant-R	0.61	ATLmed-L	ATLlat-L	0.65
11	CAU-L	LEN-L	0.60	PAR-R	PAR-L	0.65
12	CRB-L	CRB-R	0.59	AMY-L	PHGant-L	0.64
13	FRO-R	FRO-L	0.59	FRO-R	FRO-L	0.63
14	MITant-L	MITpost-L	0.58	AMY-R	PHGant-R	0.62
15	CAU-R	THA-R	0.58	STN-L	LEN-L	0.62
16	PHGpost-L	FUSpost-L	0.57	STN-R	STN-L	0.61
17	THA-R	LEN-R	0.57	STm-R	INS-R	0.61
18	STGmid-R	STGpost-R	0.56	THA-L	LEN-L	0.61
19	CAU-L	THA-L	0.56	HIP-L	AMY-L	0.61
20	ATLmed-L	ATLlat-L	0.56	STGmid-R	STGpost-R	0.60